Dielectrophoresis of DNA: Time- and Frequency-Dependent Collections on Microelectrodes

David J. Bakewell* and Hywel Morgan

***Abstract*—This paper reports measurements that characterize the collection of DNA onto interdigitated microelectrodes by high-frequency dielectrophoresis. Measurements of time-dependent collection of 12 kilobase pair plasmid DNA onto microelectrodes by dielectrophoresis show significant reduction in the response as the frequency increases from 100 kHz to 20 MHz. Collection time profiles are quantitatively measured using fluorescence microscopy over the range 100 kHz to 5 MHz and are represented in terms of two parameters: the initial dielectrophoretic collection rate, and the initial to steady-state collection transition. Measured values for both parameters are consistent with trends in the frequency-dependent real part of the effective polarizability measured for the same plasmid DNA using dielectric spectroscopy. The experimentally measured parameters are qualitatively compared with trends predicted by theory that takes into account dielectrophoretic particle movement and diffusion. The differences between experiment and theory are discussed with suggested improvements to theoretical models, for example, including the effects of electrohydrodynamically driven fluid motion.**

***Index Terms*—AC electrokinetics, dielectrophoretic collection rate, DNA concentration, nonuniform electric fields.**

I. Introduction

THERE IS considerable interest in using ac electrokinetic methods for the noncontact manipulation of DNA in microfabricated structures [1]–[4]. The envisaged applications of functionally integrated microanalytical devices in biotechnology range from "lab-on-a-chip" technology and DNA diagnostics to a wider use in genomics and proteomics [5]–[7]. An attractive ac electrokinetic method for noncontact manipulation is dielectrophoresis (DEP) which is the movement of polarizable particles in nonuniform electric fields [8]. Particle forces arise from the application of an ac voltage to microelectrodes lying within a suspension of particles in an electrolyte. The particles move under the influence of the nonuniform electric field, generated by the ac electrode potentials, depending on their effective polarizability.

Manuscript received February 22, 2005; revised September 12, 2005. *Asterisk indicates corresponding author.*

*D. J. Bakewell was with the Department of Electronics and Electrical Engineering, University of Glasgow, Glasgow G12 8LT, U.K. He is now with the Beatson Institute for Cancer Research, Bearsden G61 1BD, U.K. (e-mail: d.bakewell@beatson.gla.ac.uk).

H. Morgan was with the Department of Electronics and Electrical Engineering, University of Glasgow, Glasgow G12 8LT, U.K. He is now with the School of Electronics and Computer Science, University of Southampton, Highfield, Southampton, SO17 1BJ, U.K. (e-mail: hm@ecs.soton.ac.uk).

Digital Object Identifier 10.1109/TNB.2005.864012

Experiments over the past decade have demonstrated ways to orient, stretch, transport, and trap DNA using nonuniform fields generated in microfabricated devices [7], [9]–[12]. Dielectrophoresis has also been used as a noncontact microtool for use with DNA, including field flow fractionation [13] and molecular "surgery" [14]. Despite these novel demonstrations, often performed at high frequencies ($>$100 kHz), there has been almost no quantitative systematic characterization and analysis of high-frequency DEP collections of DNA that may find application in future microdevices.

Ajdari and Prost [15] gave theoretical predictions for trapping of DNA on microelectrodes with promising applications, but these predictions did not have experimental confirmation. Asbury *et al.* [1], [16], [17] have published quantitative studies of DNA collection onto microelectrodes by DEP at low ac frequencies. They showed that the time course of fluorescently labeled DNA trapping could be fitted by a single or double exponential profile. They compared their results against the equivalent DEP energy required to trap DNA, from which they concluded the DEP trapping efficiency was less than predicted when using values of the effective polarizability deduced from dielectric spectroscopy studies. The quantitative results of DNA trapping were performed at ac frequencies, ranging from $\sim$10 Hz to 10 kHz (typically 30 Hz) and depended on solvent conductivity and on molecular weight. Fluorescence profiles of DNA being released and diffusing away from electrode surfaces were also described.

Recently, electrode-less dielectrophoretic collections of single- and double-stranded DNA at low ac frequencies (50–1000 Hz) have been described by Chou *et al.* [2] for a range of DNA sizes, medium viscosities, and electric field strengths. In this technique, the authors used constrictions created in an insulator to create high-strength electric field gradients, and they developed a simple model for the polarization of the DNA that included electrophoretic effects to describe their experiments. However, at these low frequencies, it is difficult to ensure that the electric field in the suspending medium is independent of frequency because of substantial electrode polarization effects [18] making quantitative analysis of particle collection by DEP rather difficult [4].

In view of the importance of developing and understanding dielectrophoretic techniques for the noncontact manipulation of DNA, we report experiments on the collection of DNA plasmids at high ac frequencies. In recent work [19], [20], we reported on the DEP collection of submicrometer latex spheres onto planar interdigitated microelectrodes at high ac frequencies (0.5–5 MHz). These microspheres represent "model" colloidal particles and exhibit a well-defined particle/solvent

interface when compared with DNA macromolecules, and are more suitable for quantitative comparisons between theory and experiment. The time-dependent DEP collection of the particles was simulated using a Fokker–Planck equation (or modified diffusion) model [21] and comparisons with experiment were made.

It is likely that the success of using DEP as a new microtool for the manipulation of DNA in future microanalytical devices will depend on the ability to control the time-dependent flux. In this paper we extend our previous work [22] and describe the time-dependent DEP collection at high frequencies (100 kHz–20 MHz). Two parameters are used to characterize the experimental measurements: the initial time rate of fluorescence change, or "collection rate," and the initial to steady-state change in fluorescence. The results show that the dielectrophoretic response decreases with increasing frequency and that this is consistent with the reduction in effective polarizability measured by dielectric spectroscopy for this plasmid DNA [23], [24].

II. Experimental

The DNA was pTA250—a negatively supercoiled plasmid of $\sim 4\ \mu$m contour length. This plasmid contains a single repeat of the 8.9 kbp ribosomal RNA coding unit from wheat (*Triticum aestivum* var. Chinese Spring) subcloned into the EcoRI site of pUC19 [25]. The DNA was chosen for its mechanical robustness, suitable $\sim 1\ \mu$m size for use in DEP experiments, and the fact that its dielectric properties were known from earlier work by us [24]. The DEP collection results should be essentially independent of its precise genetic code.

The DNA plasmid was purified as outlined in [24] and stored in pure water at $-20\ ^\circ$C. The concentration of the DNA in the stock solution was estimated from the extinction coefficient at 260 nm to be 2.7 $\mu g/\mu$L. Further details of the growth, harvesting, and purification of pTA250 DNA are given in [26]. The DNA samples were fluorescently labeled with 1 mg/ml $4'$, 6-Diamidino-2-phenylindole (DAPI) (Molecular Probes, Eugene, OR, D-1306) containing 10% (v : v) 2-Mercaptoethanol (Sigma, St. Louis, MO, M3148) to decrease photobleaching and strand breakage [27]. The conductivity of the samples was measured to be 5 mS/m.

A. Fluorescence Microscopy and Quantitative DEP Measurements

A diagram of the experimental apparatus is shown in Fig. 1(a). For an experiment, 20 μL of a diluted fluorescently labeled DNA suspension (at a concentration of 0.3 $\mu g/\mu$L) was pipetted onto an interdigitated electrode array (mounted on a printed circuit board). The DNA solution was capped with a glass coverslip and the device connected to a signal source as shown. The interdigitated electrodes, shown in Fig. 1(b), were fabricated using standard photolithographic techniques [28]. They were fabricated from gold with a Ti underlayer and were 10 μm wide with a 10-μm gap.

The vertical depth-of-focus of the epi-fluorescence microscope was estimated to be $\Delta y \approx 1\ \mu$m [29]. Video images of the DNA collecting onto the electrode edges were processed using a method reported recently [20]. The software spatially averaged

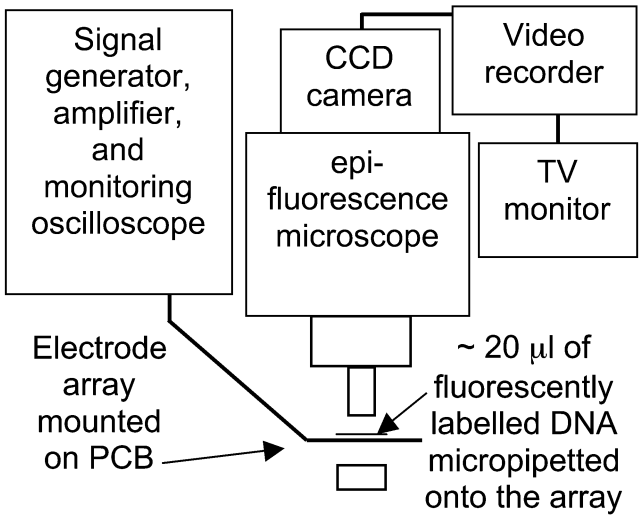

(a)

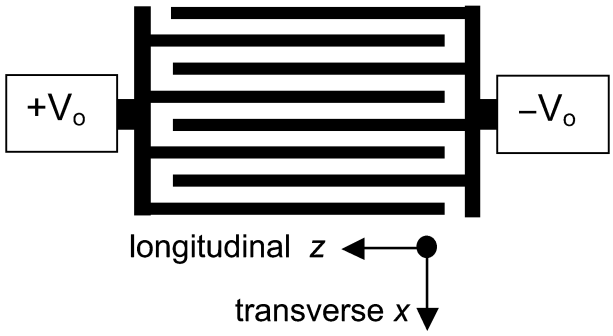

(b)

Fig. 1. (a) Schematic diagram of the experimental apparatus for monitoring the collection of DNA on the electrodes, showing ac signal source, amplifier, monitoring oscilloscope, epi-fluorescence microscope, charge-coupled device camera, video recorder, and television monitor. (b) Plan view of the planar interdigitated electrode array (not to scale) supplied with peak voltage $\pm V_0$. The electrode gap and width was 10 μm and the electrodes were typically $\sim$2 mm long. The transverse x and longitudinal z axes are as shown. The vertical y axis points upwards from the page.

pixel values of sequential video frames, utilizing the symmetric and periodic structure of the interdigitated array design. Background fluorescence outside the 1-μm depth-of-focus was removed by assuming it remains relatively unchanged during the collections, $\Delta F(t) = F(t) - F(0)$. We found this assumption to be valid, since the bulk suspension of DNA did not significantly change during the course of the experiment.

III. Theory

The movement of the DNA macromolecules throughout the suspension is governed by the deterministic DEP flux and thermally driven stochastic fluctuations (Brownian motion).

Fig. 2(a) (i) illustrates uniform macromolecule density before the onset of DEP ($t = 0$ s), and Fig. 2(a) (ii) and (iii) after DEP collections. The DEP force is spatially short-range, so that for short times $t < t_1$, as shown in Fig. 2(a) (ii), macromolecule collection around the electrodes is governed essentially by the

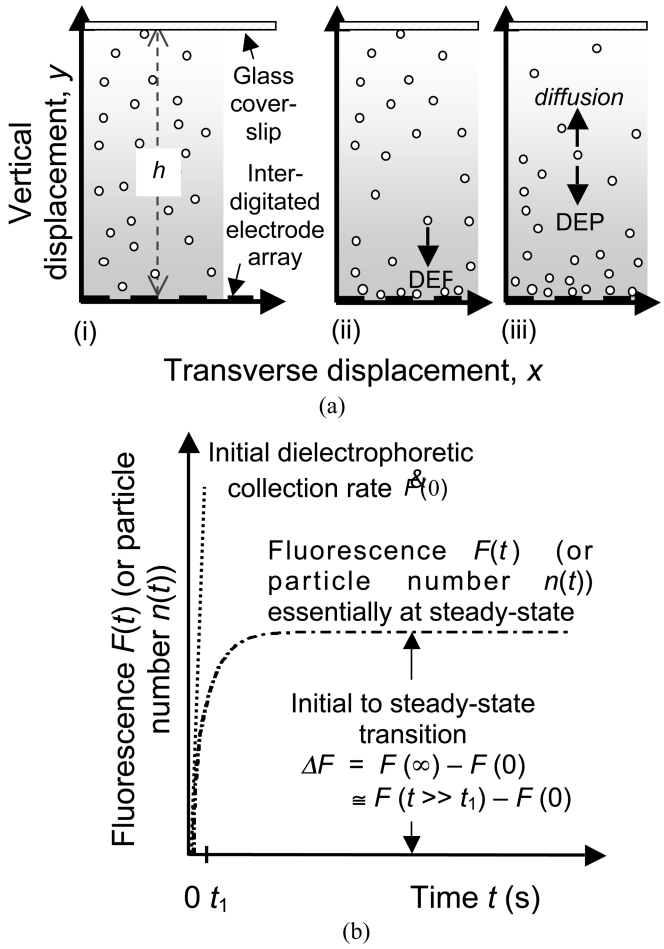

Fig. 2. (a) Diagram illustrating the one-dimensional (1-D) movement of particles between a glass coverslip (upper boundary) and planar interdigitated electrode array (lower boundary). (i) shows the distribution of particles before the onset of DEP ($t = 0$ s); (ii) shows particle collection near the electrodes under the action of DEP force ($0 < t < t_1$) giving rise to the initial collection rate; and (iii) shows particle movement governed by DEP and diffusion ($t > t_1$). (b) Graph of fluorescence intensity versus time for DNA collection on the electrode array corresponding to the 1-D particle movement shown in Fig. 2(a). The dielectrophoretic collection time profiles for the arrangement can be divided into two intervals. The observed quantity is fluorescence $F(t)$ or particle number $n(t)$. In the first interval ($0 < t < t_1$), particles collect near electrodes solely under the action of the DEP force, giving rise to the initial collection rate $\dot{F}(0)$. In the second interval ($t > t_1$) particle movement is governed by DEP and diffusion. At steady state the movement by DEP is balanced by diffusion. The initial to steady-state fluorescence change is shown as ΔF. For illustration, t_1 is the rise time where the fluorescence is 63% of the steady-state value.

deterministic DEP force. This regime of time-dependent particle collection profile is called the *initial collection rate* [8], [30]. It is given by the initial rate of change of fluorescence $\dot{F}(0)$ (or number of macromolecules detected $\dot{n}(0)$) where $\cdot$ denotes time derivative, and is depicted in Fig. 2(b).

In contrast, for $t > t_1$, shown in Fig. 2(a)(iii), diffusion of these micrometer-sized macromolecules into regions depleted by DEP influences the collection so that it is said to be diffusion limited [Fig. 2(b)]. At steady state the DEP driven particle (or macromolecule) flux is balanced by Fick's diffusion. The initial to steady-state transition in fluorescence is written as $\Delta F = F(\infty) - F(0) \cong F(t \gg t_1) - F(0)$ (or change in particle number Δn). Both $\dot{F}(0)$ and ΔF are used as key parameters in the subsequent analyzes of DEP collection profiles.

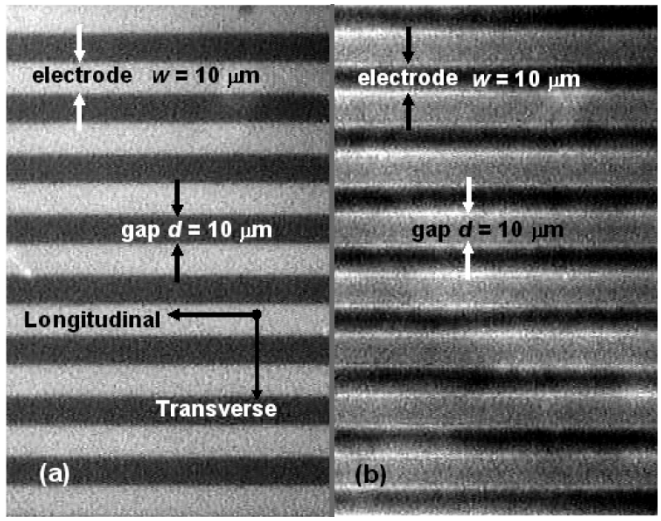

Fig. 3. Photographs showing DAPI labeled DNA plasmid suspension collecting onto the interdigitated electrode array. The images are approximately half-frame width (~60% frame height) taken from a video. (a) Array before the onset of DEP. (b) 4.2 s after onset of DEP with $V_o = 4.5$ V, $f = 200$ kHz. The gold electrodes in Fig. 3(a) appear bright because they reflect the fluorescence from the DNA suspension. In Fig. 3(b), the DNA collects between the electrodes, so the gaps appear bright.

IV. Results

Two half-frame width (~60% height) video images of the fluorescently labeled DNA suspension before and ~4 s after the onset of DEP are shown in Fig. 3(a) and (b), respectively. The electrodes reflect more light than the interelectrode glass substrate and are visible in Fig. 3(a), while Fig. 3(b) shows DNA plasmids collecting between the electrodes. The image processing software, detailed in [20], spatially averaged pixel fluorescence intensity values in 2-D (transverse and longitudinal directions). The transverse dimensions for spatial averaging across the interelectrode gap were $5 \leq x \leq 10$ μm and these average values were normalized with respect to the fluorescence intensity over the frame viewing area of the array thereby compensating for temporal fluctuations in the microscope light source. Hence, the normalized 2-D spatially averaged fluorescence intensity $F(t)$ represented time-dependent DNA plasmid collection over a representative electrode gap.

A. Quantitative Results From DEP Collection Experiments

Fig. 4 illustrates fluorescence intensity profiles $F(t)$ for one sample of DNA at different frequencies with applied peak voltage $V_o = 4.5$ V. The value of the voltage was selected to ensure a sufficiently high DNA collection rate and avoidance of fluorescence quenching while not damaging the electrodes. Data sets for other DNA samples were qualitatively similar. The average values of $F(t)$ taken from independent data sets that used the same DNA preparation, electrodes, and measurement apparatus is summarized in Table I. $F(0)$ and $F(\infty)$ are the initial and steady-state values of the normalized fluorescence intensity. Both parameters were measured by time-averaging sufficiently smooth samples of $F(t)$ before switching on the field (at $t = 0$) and afterward, typically 6–7 s (at $t \to \infty$).

The initial collection rate $\dot{F}(0)$ was determined by linear interpolation of 40 ms samples using ORIGIN 4.1 (Microcal

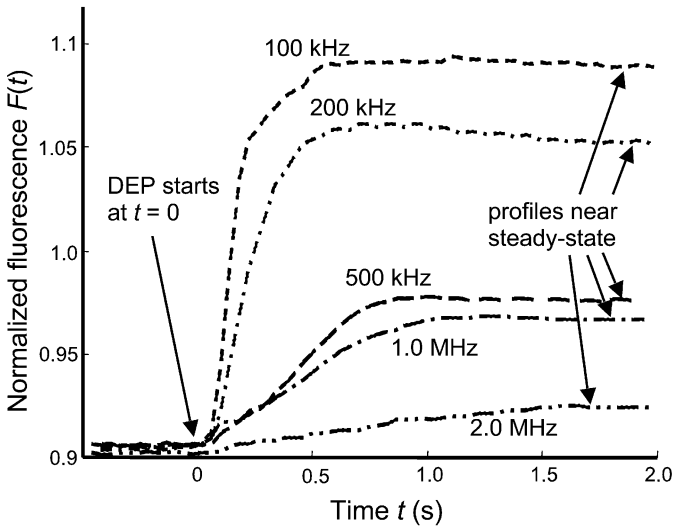

Fig. 4. Time-dependent DEP collections of pTA250 plasmid DNA for $V_o = 4.5$ V (2 1/2 second window): profiles of normalized fluorescence $F(t)$ illustrating frequency dependence of initial collection rates (gradients) plotted for different applied frequencies.

TABLE I
SUMMARY OF DIELECTROPHORETIC COLLECTION VALUES

f (MHz)	Polarizability α_m ($\times 10^{-30}$ F m^2)	No. of data sets	$F(0)$ (a.u.)	$F(\infty)$ (a.u.)	Av$\{\Delta F_r\}$ ± 1 std (%)	$\dot{F}_r(0)$ ± 1 std × 0.10
0.1	2.4	2	0.953 ± 0.017	1.137 ± 0.021	19.3 ± 0.1	8.1 ± 4.8
0.2	1.5	3	0.919 ± 0.015	1.03 ± 0.019	12.2 ± 3.5	3.7 ± 2.2
0.5	0.84	3	0.920 ± 0.016	0.992 ± 0.031	6.8 ± 1.6	1.2 ± 0.6
1	0.61	3	0.928 ± 0.021	0.985 ± 0.023	6.2 ± 0.6	0.71 ± 0.23
2	0.39	2	0.924 ± 0.031	0.963 ± 0.055	4.2 ± 2.4	0.27 ± 0.14
5	0.14	2	0.948 ± 0.02	0.962 ± 0.017	1.5 ± 0.4	0.19 ± 0.11

Parameter values obtained from the collection of DNA plasmid onto the microelectrode array ($V_o = 4.5$ V). The fluorescence intensity is given in arbitrary units (a.u.). The data show average values of repeated experiments (number of data sets listed) ± one standard deviation (denoted Av$\{\} \pm 1$ std). The repeated DEP experiments used the same DNA preparation, electrodes, and measurement apparatus. The polarizability data (column 2 from left) were obtained from experiments [24] that had a DNA volume fraction of 0.2% and suspension conductivity of 8.5 mS/m.

Software Inc., Northampton, MA). The fluorescence change is written $\Delta F = F(\infty) - F(0) \cong F(6 < t < 7) - F(0)$. Table I shows that $F(0)$ varies slightly across frequencies; hence, for quantitative analysis it is more appropriate to use the *relative* amounts of the parameters $\dot{F}_r(0) = \dot{F}(0)/F(0)$ and $\Delta F_r = \Delta F/F(0) \times 100\ (\%)$.

Two features about $\dot{F}(0)$ and ΔF (or $\dot{F}_r(0)$ and $\Delta F_r\%$) are clear from the profiles in Fig. 4 and data in Table I. First, the gradient of the initial rate of change of fluorescence $\dot{F}(0)$ decreases by about an order of magnitude as the frequency increases by a decade from 100 kHz to 1 MHz. The second feature is the decrease in the initial to steady-state fluorescence change ΔF as the frequency increases (trend can be seen more clearly as a percentage $\Delta F_r\%$).

Experiments at higher frequencies, from 10 to 20 MHz, also showed DNA collecting along the edges of the electrodes, but these accumulations were too small to be analyzed quantitatively. This confirmed the trend of a decreasing DEP force on the DNA plasmids with increasing frequency.

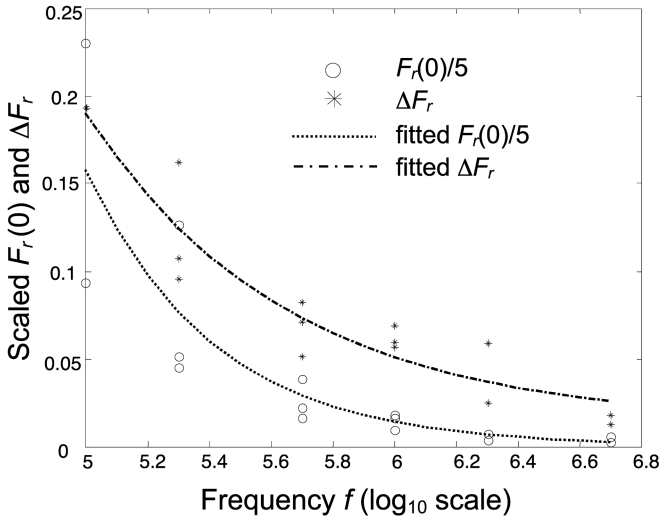

Fig. 5. Experimentally measured initial collection rate $\dot{F}_r(0)$ and initial to steady-state fluorescence ΔF_r, plotted as a function of the frequency ($\log_{10}$) of the applied electric field. For convenience the initial collection rate has been scaled by 1/5.

The experimental data summarized in Table I showing the relationship between $\dot{F}_r(0)$ and ΔF_r versus frequency are plotted in Fig. 5. Despite statistical fluctuations, mainly due to variations in the initial DNA concentration caused by aggregation, [26], both $\dot{F}_r(0)$ and ΔF_r show a clear decrease as the frequency increases, due to the reduction in the effective polarizability [31], [32] of the plasmid DNA as found using dielectric spectroscopy [24].

B. Correlations of DNA Collections With Frequency-Dependent Polarizability

The frequency-dependent real part of the effective polarizability per DNA macromolecule α_m (or dipole moment per unit electric field) required for predicting the DEP force can be found using dielectric spectroscopy [33], [34]. Values for the polarizability and corresponding relaxation times determined from previous dielectric spectroscopy measurements for the same DNA [24] were $\alpha_{m_1} = 7.88$, $\alpha_{m_2} = 1.87$, $\alpha_{m_3} = 0.197$ ($\times 10^{-30}$ F m^2), $\tau_1 = 1165$, $\tau_2 = 79.1$, and $\tau_3 = 13.7$ (ns). The frequency-dependent properties of the DNA can be modeled as the sum of three Debye dispersions given by [4], [32], and [35]

$$\alpha_m(f) \cong \mathrm{Re}\left\{\sum_{i=1}^{3} \frac{k_o \alpha_{m_i}}{(1 + j\omega\tau_i)}\right\} = \sum_{i=1}^{3} \frac{k_o \alpha_{m_i}}{(1 + \omega^2 \tau_i^2)}. \quad (1)$$

In this equation Re $\{\}$ denotes the "real part of," $j = \sqrt{-1}$, $\omega = 2\pi f$, and the coefficient k_o accounts for the orientation of the DNA subunit lengths. For a sphere with subunit lengths randomly orientated, $k_o = 1/3$. Using this expression, the data was analyzed at the same frequencies as used in the experiment $\{0.1, 0.2, 0.5, 1, 2, 5\}$ MHz to give polarizability values listed in Table I.

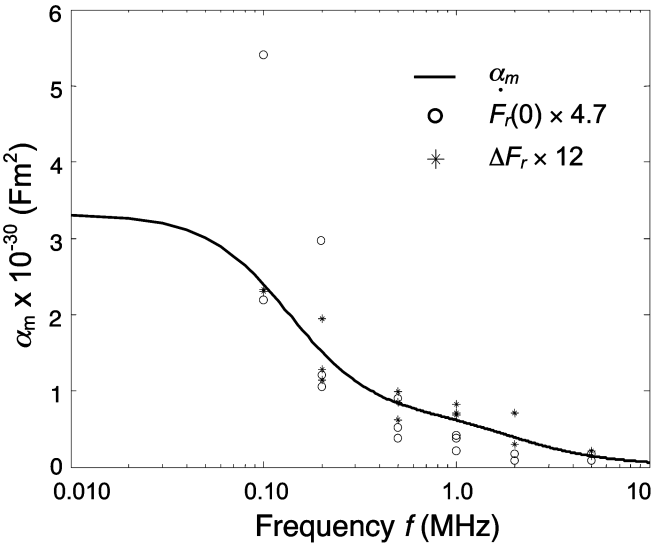

Fig. 6. Plot of the real part of the effective polarizability α_m versus frequency for the DNA (solid line) calculated from (1). The plot used experimental data from [24] that exhibited three measured dispersions for this sample of DNA. Also shown are the data points for the initial collection rate $\dot{F}_r(0)$ ($\circ$) and initial to steady-state transition ΔF_r (*). The data sets were multiplied by 4.7 and 12, respectively, conveniently chosen to illustrate the reduction in $\dot{F}_r(0)$ and ΔF_r with frequency and correlation with the polarizability.

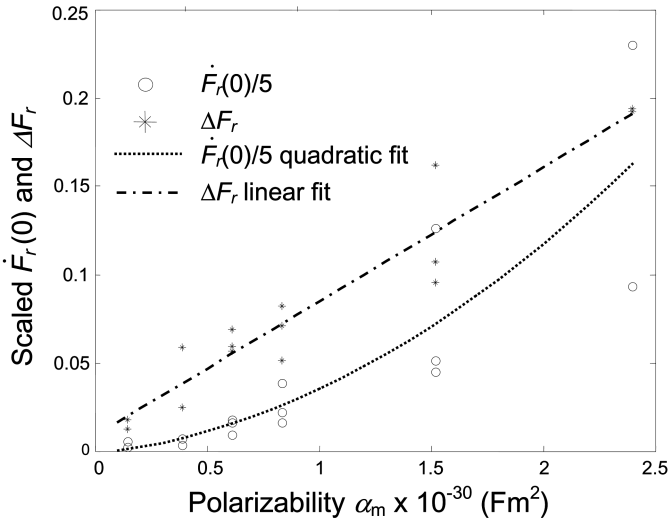

Fig. 7. Experimentally measured initial collection rate $\dot{F}_r(0)$ (scaled by a factor of 1/5), and initial to steady-state fluorescence ΔF_r versus polarizability α_m (see Fig. 6). Also shown are curves of best fit. See text for details and discussion.

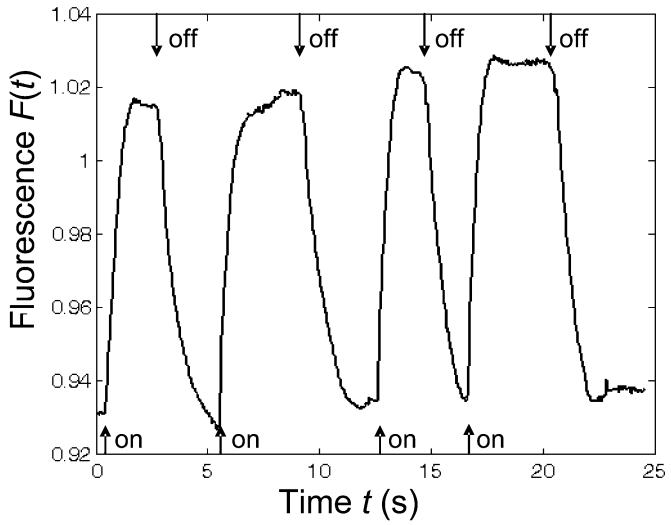

Fig. 8. Plot showing four successive DEP collections and release of DNA (due to diffusion after the DEP force was switched off, $V_o = 0$ V). The applied collection frequency was 200 kHz. The arrows show the times when the DEP force was manually switched on and off.

Fig. 6 shows the real part of the frequency-dependent polarizability for the DNA α_m calculated from (1) using the experimental values in [24]. The graph shows a characteristic polarizability function for the three dielectric dispersions measured for this DNA. Also shown in this figure are the two data sets for the parameters $\dot{F}_r(0)$ and ΔF_r which are summarized in Table I. These two data sets were multiplied by scalars (4.7 and 12 respectively) suitably chosen in order to achieve the fits shown in the figure. The figure clearly shows a correlation between the two variables $\dot{F}_r(0)$ and ΔF_r, and the reduction in the effective polarizability of the DNA with increasing frequency.

The correlation between the DEP collection parameters $\dot{F}_r(0)$ and ΔF_r and the polarizability α_m predicted from (1) is shown in Fig. 7. $\dot{F}_r(0)$ shows a nonlinear dependence that was fitted by a second-order polynomial, and ΔF_r exhibits a linear dependence on α_m.

C. Sequential DEP Collections and Relaxations

A number of DEP experiments also explored the repeatability of DEP collection and release of DNA after the DEP force is switched off ($V_o = 0$ V). Fig. 8 illustrates four successive DEP collections and release at 200 kHz. The profiles exhibited good repeatability and variations fell within the range at 200 kHz (Table I). The switching was manually controlled, so there was variation in the "on" and "off" durations. The DEP force was switched on when it was observed practically all DNA had been released from the electrodes, and off when there appeared to be no further increase in the DNA collecting on the electrodes. Successive DEP collections and release experiments were performed at different frequencies, with each cycle spanning 5–10 s. All experiments exhibited good repeatability (data not shown).

V. Discussion

The frequency dependence of the DEP collection parameters $\dot{F}_r(0)$ and ΔF_r can be explained by the widely reported frequency-dependent change in the effective polarizability α_m of DNA that has been attributed to a number of electrokinetic mechanisms [31]. In a dielectric study of pTA250 DNA [24], the polarization was mainly attributed to counterion fluctuations parallel to the longitudinal axis of the DNA [35]–[41]. In this model, counterions move freely along macromolecular DNA "subunit lengths" and are permitted to cross from one subunit to a neighboring subunit only by overcoming "potential barriers" [35], [37]. The relatively large, low-frequency relaxation at 140 kHz reported by us [24] was attributed to subunit lengths in the counterion model that were close to the Kuhn length (twice the persistence length) that is a statistical measure of DNA rigidity. The other possible mechanism applicable for the

high-frequency relaxation at 12 MHz was Maxwell–Wagner interfacial polarization [31], [42], [43]. This suggests that the most likely mechanism of induced polarizability that gives rise to the DEP force is mainly due to longitudinal movement of counterions—as described in the Mandel–Manning–Oosawa model developed in various stages by the above-referenced authors.

A. Frequency-Dependent DNA Polarizability and Dielectrophoretic Collections

The frequency dependence of the effective polarizability for DNA can be modeled as a series of Debye-like dispersions that characterize counterion movement parallel to the longitudinal axis of a macromolecule [35], cf. (1). Recently, Chou *et al.* [2] proposed a simple model for the low-frequency loss mechanism for DNA, which they used to explain the frequency-dependent DEP collection of single- and double-stranded DNA from 50 Hz to 1 kHz. Although the trapping force at low frequencies (50 Hz) was not as predicted from the Debye dispersion model, this was attributed to the presence of electrophoretic forces that were large compared with the DEP forces at such a low frequency. Asbury *et al.* [1], [17] also fitted their $\sim$10 Hz to 1 kHz frequency-dependent dielectrophoretic collections of DNA to a first order Debye dispersion and showed a relaxation frequency in the region of 100 Hz. However, in this work, we have concentrated on the high-frequency behavior of DNA, where problems due to electrophoresis and electrode polarization are eliminated.

The frequency-dependent DEP collection of plasmid DNA described in this work has shown the initial collection rate $\dot{F}_r(0)$ and the transition ΔF_r to correlate with changes in the polarizability of the DNA in the range 100 kHz to 20 MHz. In earlier work [20], we used the Fokker–Planck equation (FPE) to model particle collections, and showed that the initial particle collection rate is proportional to the polarizability. The FPE predicted $\dot{F}_r(0) \propto \alpha_m$ ($\propto$ denotes proportionality) at the onset of DEP because the effect of diffusion was assumed to be negligible under initial conditions of uniform particle concentration. Thus, only the particle flux due to DEP forces governed the initial collection rate. In contrast, the initial to steady-state transition ΔF_r predicted by the FPE was shown to exhibit a highly nonlinear, exponential dependence on α_m. The extent of the nonlinearity depended on the ratio of DEP to thermal, diffusive, energy.

B. Other Possible Factors Affecting DNA Collections

Fig. 7 shows that $\dot{F}_r(0)$ is not directly proportional to α_m as predicted by the FPE model. The relationship shown in the figure was fitted by a second-order polynomial. At this stage, there are two possible explanations for this behavior. The first pertains to the friction coefficient ζ of the plasmid DNA [44]; $\dot{F}_r(0) \propto \alpha_m$ is true if ζ remains constant and does not change with α_m (or frequency). However, if the shape of the plasmid changes under the action of a high DEP force (i.e., at low frequencies, such as 100 kHz) such that ζ is reduced, then $\dot{F}_r(0)$ will be enhanced beyond the proportional relationship. The second possibility is attributed to electrohydrodynamically (EHD) driven fluid motion, particularly ac electroosmosis. EHD tends to drag particles down from the suspension above the electrodes into the center of each electrode gap and propel them away from the electrode edge toward the center of the electrodes, and thence upwards [45]–[49]. This fluid motion tends to be stronger at lower frequencies (e.g., 100–200 kHz) and coincides with higher α_m and also the formation of plasmids that collect entirely across the gap, as shown in Fig. 3(b).

It is possible that ac electroosmosis could pull the plasmids downwards, from the suspension above the electrode gaps, thereby contributing to the initial DEP collection rate. The initial collection is observed over a very short time interval (0.1–0.2 s) as shown in Fig. 4. If the plasmids are dielectrophoretically trapped between the electrodes, so they cannot immediately escape with the upwards fluid movement above the electrodes, then the effect of ac electroosmosis would be to increase $\dot{F}(0)$. This would add to the value due solely to DEP at these lower frequencies, and possibly explain the nonlinear dependence on α_m that cannot be explained by the simple FPE model. With respect to both explanations, we note that similar DEP experiments on dilute suspensions of 216-nm-diameter latex microspheres [20] that have constant ζ collected only on the electrode edges and exhibited little interaction, and showed $\dot{F}(0)$ approximately proportional to the DEP force (i.e., α_m). A comprehensive numerical model of spatial–temporal DEP particle collections and EHD fluid motion could clarify the contribution of EHD to $\dot{F}_r(0)$.

The result that $\Delta F_r \propto \alpha_m$ shown in Fig. 7 means that the collections from initial to steady-state behave as if the DEP force is much less than predicted. This is not entirely unexpected, although there is no satisfactory explanation for this observation at present. Essentially, FPE simulations by us using the experimental applied peak voltage and typical values for other parameters predicted that ΔF_r should exhibit a highly nonlinear dependence on α_m and the DEP force should be strong enough to attract practically all of the suspended of DNA onto the electrode array (data not shown). However, only very modest collections of DNA on the array were observed in these experiments and very little depletion was evident in the bulk suspension. These observations are consistent with DEP collection experiments using 216-nm-diameter latex microspheres [19], [20], [26].

There are a number of electrokinetic mechanisms that could reduce the DEP force acting on plasmid DNA. One possibility is that the temporal accumulation of negatively charged DNA and counterions near the electrodes, as illustrated in Fig. 3(b), could alter the electric field distribution and reduce the DEP force. Counterion presence is not taken into account in current DEP force evaluations that are based on Laplace's equation that assumes zero charge density [50]–[52]. Another possible reason for the strength of the DEP force being weaker than predicted for regions close to the electrode edges, is that the polarizability could saturate at high strength electric fields [17], [40]. Particle levitation experiments by Markx *et al.* [53] and Cui *et al.* [54] have shown that the actual field experienced by the particles is close to the theoretical value in the far field at these frequencies, so it is unlikely that electrode polarization would be a factor that reduces the DEP force.

An alternative explanation to the reduction in DEP force is that there is an additional force that acts against DEP or sufficiently disrupts the quasi-steady state collection of plasmids, so they do not all collect on the array. The most likely of these is

ac electroosmosis, which produces rolls in the fluid that can extend far above the electrode array. Since they involve both upwards and downwards fluid movement, their net effect would need to be taken into account. As with $\dot{F}_r(0)$, a comprehensive numerical model of DEP and EHD motion is needed that would completely explain the behavior of ΔF_r. Incorporation of fluid motion may also assist analysis and theoretical comparisons of further collection experiments that use a range of applied voltages and medium conductivities—provided these parameters are constrained to avoid problems, such as electrode damage and fluorescence quenching.

Despite the much-needed improvements that could theoretically predict DEP collections of DNA, the frequency dependence and repeatability described in this paper may find useful application in future microdevices. In general, we have noted that for many DEP studies using both DNA and 216-nm-diameter latex beads, for any given experiment, once the first DEP collection and release has been performed, successive collections and release show good repeatability.

VI. Conclusion

Fluorescence microscopy was used to measure dielectrophoretic collections of pTA250 plasmid DNA onto 10-μm-width 10-μm-gap planar interdigitated electrodes as a function of frequency. Collection time profiles were quantified by two parameters: the initial DEP collection rate and initial to steady-state transition. The parameter values exhibited a clear decrease as the frequency increased from 100 kHz to 20 MHz. The decrease in frequency response was consistent with a reduction in the real part of the effective polarizability of the plasmid DNA measured by dielectric spectroscopy. Correlations of these two parameters with the DNA polarizability show a need to improve current models of DEP collections, particularly with reference to electrohydrodynamically driven fluid motion that confounds measurements. Other factors also include modeling the effect of DNA accumulation on the electric field nonuniformity. Successive DEP collection and release showed good repeatability, and this feature, together with the frequency dependence, may be useful for controlling noncontact movement of DNA.

Acknowledgment

The authors would like to thank Drs J. J. Milner, E. Cecchini, and P. J. Dominy for assistance with preparation of the DNA, and Drs. I. Ermolina and N. Green for helpful advice and discussions. D. J. Bakewell would also like to thank the University of Glasgow and the CVCP Overseas Research Student Awards Scheme.

References

[1] C. L. Asbury, A. H. Diercks, and G. van den Engh, "Trapping of DNA by dielectrophoresis," *Electrophoresis*, vol. 23, pp. 2658–2666, 2002.

[2] C.-F. Chou, J. O. Tegenfeldt, O. Bakajin, S. S. Chan, E. C. Cox, N. Darnton, T. Duke, and R. H. Austin, "Electrodeless dielectrophoresis of single- and double- stranded DNA," *Biophys. J.*, vol. 83, pp. 2170–2179, 2002.

[3] R. Hölzel, N. Gajovic-Eichelmann, and F. F. Bier, "Oriented and vectorial immobilization of linear M12 dsDNA between interdigitated electrodes—toward single molecule DNA nanostructures," *Biosensors and Bioelectronics*, vol. 18, pp. 555–564, 2003.

[4] H. Morgan and N. Green, *AC Electrokinetics: Colloids and Nanoparticles*. Baldock, UK: Research Studies, 2003.

[5] S. Abramowitz, "Toward inexpensive DNA diagnostics," *Trends Biotechnol.*, vol. 14, pp. 397–401, 1996.

[6] J. Cheng, E. L. Sheldon, L. Wu, A. Uribe, L. O. Gerrue, J. Carrino, M. J. Heller, and J. P. O'connell, "Preparation and hybridization analysis of DNA/RNA from E. Coli on microfabricated bioelectronic chips," *Nature Biotechnol.*, vol. 16, pp. 541–546, 1998.

[7] S. M. Crippen, M. R. Holl, and D. R. Meldrum, "Examination of dielectrophoretic behavior of DNA as a function of frequency from 30 Hz to 1 MHz using a flexible microfluidic test apparatus," in *Proc. Micro Total Analysis Systems 2000*A. van den Berg, W. Olthius, and P. Bergveld, Eds., pp. 529–532.

[8] H. A. Pohl, *Dielectrophoresis*. Cambridge, U.K.: Cambridge Univ. Press, 1978.

[9] M. Washizu and O. Kurosawa, "Electrostatic manipulation of DNA in microfabricated structures," *IEEE Trans. Ind. Appl.*, vol. 26, no. 6, pp. 1165–1172, Nov./Dec. 1990.

[10] ——, "Applications of electrostatic stretch-and-positioning of DNA," *IEEE Trans. Ind. Appl.*, vol. 31, no. 3, pp. 447–456, 1995.

[11] A. Mizuno, M. Nishioka, T. Tanizoe, and S. Katsura, "Handling of a single DNA molecule using electric field and laser beam," *IEEE Trans. Ind. Appl.*, vol. 31, no. 6, pp. 1452–1457, Nov./Dec. 1995.

[12] K. Morishima, T. Fukuda, F. Arai, H. Matsuura, and K. Yoshikawa, "Noncontact transportation of DNA molecule by dielectrophoretic force for micro DNA flow system," in *Proc. IEEE Int. Conf. Robotics and Automation*, 1996, pp. 2214–2219.

[13] M. Washizu, S. Suzuki, O. Kurosawa, T. Nishizaka, and T. Shinohara, "Molecular dielectrophoresis of biopolymers," *IEEE Trans. Ind. Appl.*, vol. 30, no. 4, pp. 835–843, Jul./Aug. 1994.

[14] T. Yamamoto, M. Washizu, O. Kurosawa, and N. Shimamoto, "Molecular surgery of DNA," *Proc. SPIE, Int. Soc. Opt. Eng. USA*, vol. 3202, pp. 228–236, 1998.

[15] A. Ajdari and J. Prost, "Free-flow electrophoresis with trapping by a transverse inhomogeneous field," *Proc. Nat. Acad. Sci. USA*, vol. 88, pp. 4468–4471, 1991.

[16] C. L. Asbury and G. van den Engh, "Trapping of DNA in nonuniform oscillating electric fields," *Biophys. J.*, vol. 74, pp. 1024–1030, 1998.

[17] C. L. Asbury, "Manipulation of DNA Using Nonuniform Oscillating Electric Fields," Ph.D. dissertation, Univ. Washington, Seattle, 1999.

[18] H. P. Schwan, "Electrode polarization impedance and measurements in biological materials," *Ann. New York Acad. Sci.*, vol. 148, pp. 191–209, 1968.

[19] D. J. Bakewell and H. Morgan, "Measuring the frequency dependent polarizability of colloidal particles from dielectrophoretic collection data," *IEEE Trans. Dielectr. Electr. Insul.*, vol. 8, no. 3, pp. 566–571, Jun. 2001.

[20] ——, "Quantifying dielectrophoretic collections of sub-micron particles on microelectrodes," *Meas. Sci. Technol.*, vol. 15, no. 3, pp. 254–266, 2004.

[21] C. W. Gardiner, *Handbook of Stochastic Methods for Physics, Chemistry, and the Natural Sciences*. Berlin, Germany: Springer-Verlag, 1985.

[22] D. Bakewell, H. Morgan, and J. J. Milner, "Characterization of the dielectrophoretic movement of DNA in micro-fabricated structures," in *Proc. 10th Int. Conf. Electrostatics*, 1999, pp. 73–76.

[23] Yu. D. Feldman, A. Andrianov, E. Polygalov, I. Ermolina, G. Romanychev, Y. Zuev, and B. Milgotin, "Time domain dielectric spectroscopy: An advanced measuring system," *Rev. Sci. Instrum.*, vol. 67, pp. 3208–3216, 1996.

[24] D. Bakewell, I. Ermolina, H. Morgan, J. Milner, and Y. Feldman, "Dielectric relaxation measurements of 12 kbp plasmid DNA," *Biochem. Biophys. Acta*, vol. 1493, pp. 151–158, 2000.

[25] W. L. Gerlach and J. R. Bedbrook, "Cloning and characterization of ribosomal RNA genes from wheat and barley," *Nucleic Acids Res.*, vol. 7, pp. 1869–1885, 1979.

[26] D. J. G. Bakewell, "Dielectrophoresis of colloids and polyelectrolytes," Ph.D. dissertation, Univ. Glasgow, Glasgow, U.K., 2002.

[27] M. Yanagida, Y. Hiraoka, and I. Katsura, "Dynamic behaviors of DNA molecules in solution studied by fluorescence microscopy," *Cold Spring Harbor Symp. Q. Biol.*, vol. 47, pp. 177–187, 1983.

[28] J. Pacansky and J. R. Lyerla, "Photochemical decomposition mechanisms for AZ-type photoresists," *IBM. J. Res. Develop.*, vol. 23, no. 1, pp. 42–55, 1979.
[29] H. Piller, *Microscope Photometry*. Berlin, Germany: Springer-Verlag, 1977.
[30] P. R. C. Gascoyne, J. Noshari, F. F. Becker, and R. Pethig, "Use of dielectrophoretic collection spectra for characterizing differences between normal and cancerous cells," *IEEE Trans. Ind. Appl.*, vol. 30, no. 4, pp. 829–833, 1994.
[31] S. Takashima, *Electrical Properties of Biopolymers and Membranes*. Philadelphia, PA: Adam Hilger, 1989.
[32] S. Bone and C. A. Small, "Dielectric studies of ion fluctuation and chain bending in native DNA," *Biochim. Biophys. Acta*, vol. 1260, pp. 85–93, 1995.
[33] X.-B. Wang, Y. Huang, R. Hölzel, J. P. H. Burt, and R. Pethig, "Theoretical and experimental investigations of the interdependence of the dielectric, dielectrophoretic and electrorotational behavior of colloidal particles," *J. Phys. D, Appl. Phys.*, vol. 26, pp. 312–322, 1993.
[34] X.-B. Wang, Y. Huang, F. F. Becker, and P. R. C. Gascoyne, "A unified theory of dielectrophoresis and travelling wave dielectrophoresis," *J. Phys. D, Appl. Phys.*, vol. 27, pp. 1571–1572, 1994.
[35] F. van der Touw and M. Mandel, "Dielectric increment and dielectric dispersion of solutions containing simple charged linear macromolecules," *Biophys. Chem.*, vol. 2, pt. 1 and 2, pp. 218–241, 1974.
[36] M. Mandel, "The electric polarization of rod-like, charged macromolecules," *Mol. Phys.*, vol. 4, pp. 489–496, 1961.
[37] ——, "Dielectric properties of charged linear macromolecules with particular reference to DNA," *Ann. New York Acad. Sci.*, vol. 303, pp. 74–87, 1977.
[38] G. S. Manning, "The molecular theory of polyelectrolyte solutions with applications to the electrostatic properties of polynucleotides," *Q. Rev. Biophys.*, vol. 11, no. 2, pp. 179–246, 1978.
[39] ——, "Limiting laws and counterion condensation in polyelectrolyte solutions V. Further development of the chemical model," *Biophys. Chem.*, vol. 9, pp. 65–70, 1978.
[40] ——, "A condensed counterion theory for polarization of polyelectrolyte solutions in high fields," *J. Chem. Phys.*, vol. 99, no. 1, pp. 477–486, 1993.
[41] F. Oosawa, *Polyelectrolytes*. New York: Marcel Dekker, 1971.
[42] B. Saif, R. K. Mohr, C. J. Montrose, and T. A. Litovitz, "On the mechanism of dielectric relaxation in aqueous DNA solutions," *Biopolymers*, vol. 31, pp. 1171–1180, 1991.
[43] C. Grosse, "Microwave absorption of suspensions of DNA type particles in electrolyte solution," *Alta Frequenza*, vol. 58, pp. 365–368, 1989.
[44] T. Odijk, "Sedimentation of DNA supercoils and bacterial nucleoids," *Colloids Surf. A, Physicochem. Eng. Aspects*, vol. 120, pp. 191–197, 2002.
[45] D. J. Tritton, *Physical Fluid Dynamics*. Oxford, U.K.: Oxford Univ. Press, 1988.
[46] A. Ramos, H. Morgan, N. G. Green, and A. Castellanos, "AC electrokinetics: a review of forces in microelectrode structures," *J. Phys. D, Appl. Phys.*, vol. 31, pp. 2338–2353, 1998.
[47] ——, "AC electric-field-induced fluid flow in microelectrodes," *J. Colloid Interface Sci.*, vol. 217, pp. 420–422, 1999.
[48] N. G. Green, A. Ramos, A. Gonzalez, H. Morgan, and A. Castellanos, "Fluid flow induced by nonuniform AC electric fields in electrolytic solutions on micro-electrodes. Part I: Experimental measurements," *Phys. Rev. E*, vol. 61, pp. 4011–4018, 2000.
[49] N. G. Green, A. Ramos, and H. Morgan, "AC electrokinetics: A survey of sub-micrometer particle dynamics," *J. Phys. D, Appl. Phys.*, vol. 33, pp. 632–641, 2000.
[50] J. D. Jackson, *Classical Electrodynamics*, 2nd ed. New York: Wiley, 1975.
[51] H. Morgan, G. Izquierdo, D. Bakewell, N. G. Green, and A. Ramos, "The dielectrophoretic and travelling wave forces for interdigitated electrode arrays: Analytical solution using Fourier series," *J. Phys. D, Appl. Phys.*, vol. 34, pp. 1553–1561, 2001.
[52] ——, "The dielectrophoretic and travelling wave forces for interdigitated electrode arrays: analytical solution using Fourier series (erratum)," *J. Phys. D, Appl. Phys.*, vol. 34, no. 1, 2001.
[53] G. H. Markx, R. Pethig, and J. Rousselet, "The dielectrophoretic levitation of latex beads, with reference to field-flow fractionation," *J. Phys. D, Appl. Phys.*, vol. 30, pp. 2470–2477, 1997.
[54] L. Cui, D. Holmes, and H. Morgan, "The dielectrophoretic levitation and separation of latex beads in microchips," *Electrophoresis*, vol. 22, pp. 3893–3901, 2001.

David J. Bakewell received the B.E.E. degree in electrical engineering (first-class honors) from the University of Melbourne in 1983 and the Ph.D. degree from the University of Glasgow in 2003 for his research on dielectrophoresis of colloids and polyelectrolytes.

He joined the Australian Telecommunications Commission in 1984, and from 1985–1996 he conducted research into the performance of radio and optical fiber digital transmission systems and networks. He is currently at the Beatson Cancer Research Laboratories, Bearsden, U.K., where he is developing statistical methods for improving microarray gene expression estimation. His research interests also include developing methods for noncontact manipulation of nanoscale particles and DNA.

Hywel Morgan received the B.Sc. degree in electronic engineering and the Ph.D. in electronic engineering from the University of Wales, Bangor, U.K., in 1981 and 1985, respectively.

He was appointed to a lectureship at the University of Glasgow in 1993, where he established a research program in ac electrokinetics. He was appointed professor of Bioelectronics at the University of Glasgow in 2001, and is now Professor of Bioelectronics at the University of Southampton, Southampton, U.K. He recently coauthored a text-book, *AC Electrokinetics: Colloids and Nanoparticles* (Research Studies Press, 2003). His research interests are concerned with understanding and exploiting the applications of electric fields to biology, particularly in the context of micro- and nanosystems. He has developed new bioparticle manipulation and characterization methods and is interested in developing methods for controlling fluids in microsystems through the exploitation of electrohydrodynamic effects. He is a member of the editorial board of the *Journal of Electrostatics* and the *IEE Proceedings on Nanobiotechnology*.

Prof. Morgan was awarded a Royal Society-Leverhulme Senior Research Fellowship in 2001.